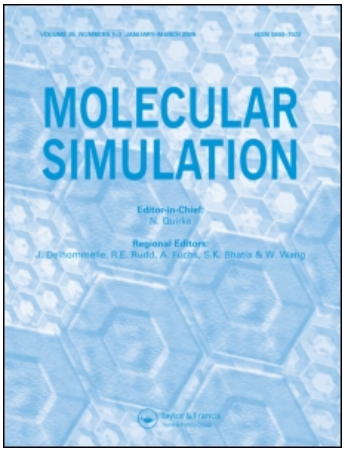

Molecular Simulation
Publication details, including instructions for authors and subscription information:
http://www.informaworld.com/smpp/title~content=t713644482

FT-IR, FT-Raman and UV-vis spectra and quantum chemical investigation of trimetazidine

R. Meenakshi[a]; Lakshmi Jagannathan[a]; S. Gunasekaran[b]; S. Srinivasan[c]
[a] Department of Physics, C.T.T.E. College for Women, Chennai, India [b] PG and Research Department of Physics, Pachaiyappa's College, Chennai, India [c] Department of Physics, L.N. Government College, Ponneri, India

Online publication date: 04 November 2010

To cite this Article Meenakshi, R. , Jagannathan, Lakshmi , Gunasekaran, S. and Srinivasan, S.(2010) 'FT-IR, FT-Raman and UV-vis spectra and quantum chemical investigation of trimetazidine', Molecular Simulation, 36: 12, 969 — 977
To link to this Article: DOI: 10.1080/08927022.2010.497925
URL: http://dx.doi.org/10.1080/08927022.2010.497925

Molecular Simulation
Vol. 36, No. 12, October 2010, 969–977

Taylor & Francis
Taylor & Francis Group

FT-IR, FT-Raman and UV–vis spectra and quantum chemical investigation of trimetazidine

R. Meenakshi[a], Lakshmi Jagannathan[a], S. Gunasekaran[b1] and S. Srinivasan[c]*

[a]*Department of Physics, C.T.T.E. College for Women, Chennai 600 011, India;* [b]*PG and Research Department of Physics, Pachaiyappa's College, Chennai 600 030, India;* [c]*Department of Physics, L.N. Government College, Ponneri 601 204, India*

(*Received 22 March 2010; final version received 13 May 2010*)

Fourier transform infrared and Raman spectra of trimetazidine (TMZ) were recorded. The structure, geometry optimisation and vibrational frequencies were investigated. The specific mode of normal coordinate analysis was made for the stable conformer of the molecule using restricted Hartree–Fock (RHF) and density functional theory (DFT) calculations (B3LYP) with the 6-31G(d,p) basis set. Comparison of the observed fundamental vibrational frequencies of the molecule and calculated results by RHF and DFT methods indicates that B3LYP is superior to molecular vibrational problems. The thermodynamic functions of the title molecule were also calculated using the RHF and DFT methods. The DFT-optimised geometry was used in the time-dependent DFT and ZINDO calculations to predict the oscillator strength, electronic transition energies between the orbital and wavelength of the transitions. The DFT-based NMR calculation procedure was used to assign the ^{1}H NMR chemical shift of TMZ. The electron density-based local reactivity descriptors such as Fukui functions were calculated to explain the chemical selectivity or reactivity site in TMZ.

Keywords: FT-IR; FT-Raman; UV–vis; ^{1}H NMR spectrum and trimetazidine

1. Introduction

Trimetazidine (TMZ) [1-(2,3,4-trimethoxybenzyl)-piperazine] is an effective, well-tolerated drug mainly used in angina pectoris. In addition to the vasodilatory effects on the coronary arteries, beneficial results with TMZ treatment in patients with ischaemic heart disease and heart failure are well documented. Favourable effects of TMZ are reported on other ischaemic organs as well. Several mechanisms were suggested to be responsible for these effects, such as a reduction in reactive oxygen species, alteration in cellular lipid composition and inhibition of mitochondrial fatty acid oxidation [1]. TMZ is one of the partial free fatty acid oxidation inhibitors which has shown to provide beneficial effects on the ischaemic heart without altering central haemodynamics or baseline contractile parameters as observed with traditional antianginal drug therapy. TMZ has demonstrated antianginal properties via manipulation of cardiac metabolism in animal models and in humans [2–6]. Inci et al. [7] showed that TMZ is an anti-ischaemic drug which restores the ability of ischaemic cells to produce energy and reduces the generation of oxygen-derived free radicals. They also suggest that TMZ may be an important adjunct in the prevention of post-transplant drug ischaemia-reperfusion injury. Clinically, TMZ decreases ischaemia during coronary angioplasty [8] and cardiac surgery [9], and there is clear evidence that it can improve exercise tolerance in patients with coronary artery disease [10] and shows an efficacy similar to that of propranolol [3] or nifedipine [2]. Most of the knowledge gathered so far to that of shows that the title molecule is of considerable interest in the field of medicine and pharmaceutical science. Hence, the present study is devoted to performing a detailed calculation of the molecular structure as well as to predicting the infrared spectra and chemical reactivity sites of the title molecule.

2. Experimental

A spectroscopic pure sample of TMZ was procured from a reputed pharmaceutical firm in Chennai, India, and used as such without further purification. The FT-IR spectrum of TMZ was recorded with ABB Bomem Series spectrometer over the region 4000-400 cm^{-1} by adopting KBr pellet technique at Dr Ceeal Analytical Lab, Chennai, India. The FT-Raman spectrum was recorded at Central Electro Chemical Research Institute Laboratory, Karaikudi, India, with Nexus 670 spectrometer. The laser frequency of 15,798 cm^{-1} was used as excitation source. The spectrometer is fitted with XT-KBr beam splitter and a deuterated triglycine sulfate (DTGS) detector. A base line correction was made for the spectrum recorded.

3. Computation

All the theoretical computations were performed at restricted Hartree–Fock (RHF) and B3LYP levels on a Pentium IV/1.6 GHz personal computer using the Gaussian 03W program package [11]. The geometries

*Corresponding author. Email: dr_s_srinivasan@yahoo.com

ISSN 0892-7022 print/ISSN 1029-0435 online

DOI: 10.1080/08927022.2010.497925
http://www.informaworld.com

were first optimised at the RHF level of theory employing 6-31G(d,p) basis set. Density functional theory (DFT) with three-parameter hybrid functional (B3) [12] for the exchange part and the LYP correlation function [13] for the computation of vibrational spectra and energies of optimised structure were used. Polarisation functions were added for better description of polar bonds. The optimised geometry was used in the vibrational frequency calculations at the RHF and DFT levels to characterise all stationary points as minima. Finally, the calculated normal mode vibrational frequencies provide thermodynamic properties by way of statistical mechanics. The vibrational frequency assignments were made with a high degree of accuracy with the help of Chemcraft software program [14]. The individual atomic charges calculated by Mulliken population analysis (MPA) were used to calculate Fukui function and local softness as proposed by Yang and Mortier [15] and Parr and Yang [16].

4. Results and discussion

4.1 Molecular geometry

The optimised geometry of TMZ, obtained by the DFT and RHF levels of calculation, is provided in Tables 1 and 2 in accordance with the atom numbering scheme given in Figure 1. Tables 1 and 2 compared the bond lengths and bond angles, respectively, for TMZ with those experimentally available from X-ray diffraction data [17]. From the calculated values, it is observed that most of the optimised bond lengths are slightly larger than the experimental values. This is due to the fact that the calculations were done on single molecule in the gaseous state contrary to the experimental values recorded in the presence of intermolecular interactions. Comparing bond lengths using DFT (B3LYP) with those using RHF, as a whole, the former is larger than the latter and the B3LYP-calculated values correlate fairly compared with the experimental results. Although they are slight differences, calculated geometric parameters represent a good approximation, and they are the base for calculating other parameters, such as vibrational frequencies, NMR chemical shifts, and atomic charges.

4.2 Vibrational band assignment

TMZ minimum energy structure belongs to the C1 symmetry point group. We have assigned the fundamental modes of TMZ on the basis of group (i.e. methyl, methylene, piperazine and benzene) vibrational concept and calculated vibrational frequencies. The FT-IR and FT-Raman spectra of TMZ are given in Figures 2 and 3, respectively. The principal peaks are provided in Table 3. It is noticed that the best representation of low frequency region IR spectrum is obtained in both the methods. From Table 3, both B3LYP and RHF produce the same result which agree with the experimental values. It is well known that theoretically calculated harmonic vibrational frequencies are typically overestimated by over 10% than the experimentally observed fundamentals. Errors arise because of the neglect of anharmonicity and electronic correlation and the use of finite basis set. Scaling factors are usually applied to the force constants to obtain a good agreement between the calculated and observed fundamentals. However, the scaling factors 0.960 and 0.899 for

Table 1. Selected bond length (Å) values for TMZ.

Bond length	B3LYP	RHF	Exp.	Bond length	B3LYP	RHF	Exp.	Bond length	B3LYP	RHF	Exp.
R(1–2)	1.464	1.453	1.49	R(7–8)	1.526	1.526		R(11–12)	1.392	1.382	
R(1–6)	1.461	1.451	1.49	R(8–9)	1.411	1.394		R(11–14)	1.381	1.361	1.37
R(1–7)	1.469	1.454	1.51	R(8–13)	1.398	1.389		R(12–13)	1.393	1.382	
R(2–3)	1.534	1.526		R(9–10)	1.41	1.395		R(14–15)	1.433	1.411	1.44
R(3–4)	1.467	1.454	1.52	R(9–18)	1.371	1.360	1.39	R(16–17)	1.435	1.412	1.45
R(4–5)	1.466	1.452	1.48	R(10–11)	1.408	1.391		R(18–19)	1.428	1.406	1.43
R(5–6)	1.536	1.527		R(10–16)	1.38	1.359	1.38				

Table 2. Selected bond angle (°) values for TMZ.

Bond angle	B3LYP	RHF	Exp.	Bond angle	B3LYP	RHF	Exp.	Bond angle	B3LYP	RHF	Exp.
A(2–1–6)	111.6	111.9	112.3	A(7–8–9)	121.2	121.5		A(9–18–19)	120.0	117.6	113.5
A(2–1–7)	114.6	115.1	111.7	A(7–8–13)	120.4	120.5		A(11–10–16)	120.8	121.3	120.0
A(1–2–3)	109.8	109.7	111.0	A(9–8–13)	118.4	118.0		A(10–11–12)	120.4	120.1	
A(6–1–7)	114.5	115.1	110.3	A(8–9–10)	120.5	121.0		A(10–11–14)	120.4	120.4	117
A(1–6–5)	110.0	109.8	109.0	A(8–9–18)	116.6	118.9	116.0	A(10–16–17)	115.7	117.0	113.9
A(1–7–8)	117.4	117.5	115.9	A(8–13–12)	121.8	121.6		A(12–11–14)	119.2	119.6	121
A(2–3–4)	113.6	113.2	108.0	A(10–9–18)	122.9	120.0	121.0	A(11–12–13)	119.5	119.8	
A(3–4–5)	110.4	111.1	109.0	A(9–10–11)	119.4	119.4		A(11–14–15)	114.2	115.1	120
A(4–5–6)	113.6	113.1	112.0	A(9–10–16)	119.6	119.2	119.0				

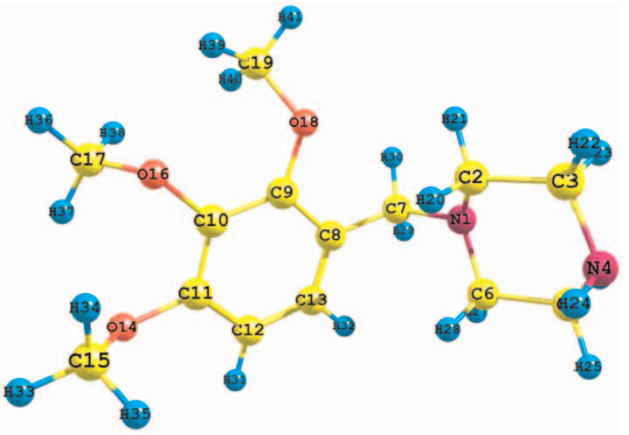

Figure 1. Atom numbering adopted in this study for TMZ.

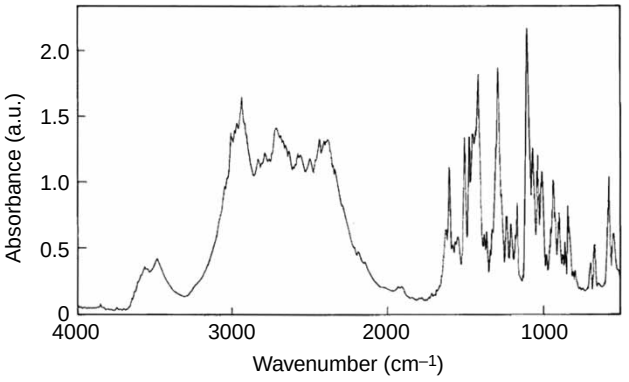

Figure 2. FT-IR spectrum of TMZ.

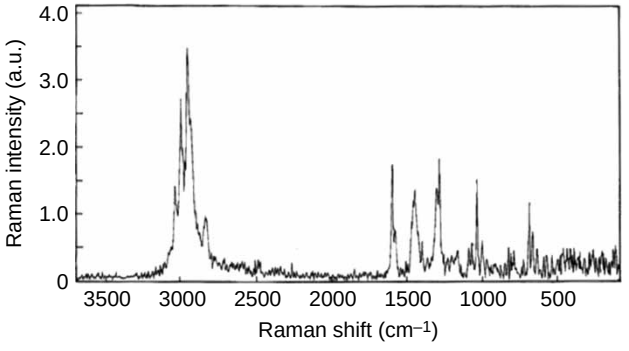

Figure 3. FT-Raman spectrum of TMZ.

DFT and RHF values, respectively, have to be necessarily used to find a good agreement with the experimental values [18]. The DFT values were found to be in good agreement with the experimental values after scaling the vibrational frequencies in comparison to RHF values.

4.2.1 N—H vibrations

Heterocyclic compounds containing an N—H group exhibit N—H stretching absorption in the region from 3500 to 3200 cm^{-1} [19] which depends on the degree of hydrogen bonding and hence upon the physical state of the sample [20]. The N—H bond present in the TMZ will give rise to N—H stretching, in-plane and out-of-plane bending deformations. In general, N—H stretching vibrations are sharper and weaker and do not occur as wide and broad O—H stretching vibrations. In the present study, the FT-IR bands at 3486 cm^{-1}, the RHF-scaled frequency calculated band at 3335 cm^{-1} and B3LYP-scaled frequency band at 3349 cm^{-1} were assigned to N—H stretching vibration. The FT-IR band at 1546 cm^{-1} was assigned to in-plane bending modes of N—H. The corresponding N—H in-plane bending vibration is predicted at 1449 and 1356 cm^{-1} in B3LYP and RHF methods, respectively. The N—H out-of-plane bending vibration predicted at 860 cm^{-1} in B3LYP and 794 cm^{-1} in RHF levels of calculations is absent in both IR and Raman spectra.

4.2.2 C—H vibrations

The hetero aromatic structure shows the presence of C—H stretching vibrations in the region 3100–3000 cm^{-1}, which is the characteristic region for the ready identifications of the C—H stretching vibrations [21]. In this region, the bands are not affected by the nature of the substituent. Hence, in the present study, the FT-IR band at 3007 and FT-Raman band at 3008 cm^{-1} are assigned to C—H stretching vibration. Three methoxy groups present in the title molecule exhibit nine C—H stretching modes of vibrations. These vibrations are identified and presented in the Table 2. Also, the C—H stretching mode of vibrations due to methylene and piperazine ring is also identified and presented. Krishnakumar and Seshadri [22] identified the strong C—H stretching absorption of methylene group centred on 2925 cm^{-1}. In the present study, the B3LYP-calculated C—H stretching absorption of methylene group bands is in good agreement with the experimental and literature value. The in-plane and out-of-plane bending vibrations due to C—H modes were identified for the title compound and they are presented in Table 2.

4.2.3 C—O vibrations

The C—C vibration could interact with the C—O if it was of the same species, but generally it is not. The experimental frequencies at 1168 cm^{-1} in both IR and Raman spectra of the title molecule are assigned to C—O stretching vibrations. This is in excellent agreement with B3LYP-predicted frequency at 1168 cm^{-1} [23]. The O—CH_3 mode is assigned in the region 1000–1100 cm^{-1} for anisole and its derivatives [24]. In this work, the O—CH_3 stretching mode is assigned to medium weak IR band at 1040 cm^{-1} and to Raman band at 1041 cm^{-1}. The theoretically computed B3LYP value closely coincides with the experimental results. The same

Table 3. Observed and calculated IR wave numbers (cm^{-1}) for TMZ.

	Unscaled wave numbers		Scaled wave numbers		Exp. wave numbers		
S.no.	B3LYP	RHF	B3LYP	RHF	FT-IR	FT-Raman	Assignment
1	3478	3748	3349	3335	3486		N—H stretching
2	3212	3374	3093	3002			C—H stretching (benzene ring)
3	3185	3350	3067	2981	3060		C—H stretching (benzene ring)
4	3154	3312	3037	2947			C—H stretching (methyl group)
5	3145	3301	3028	2937	3115		C—H stretching (methyl group)
6	3144	3298	3027	2935			C—H stretching (methyl group)
7	3118	3277	3002	2916	3007		C—H stretching (methyl group)
8	3116	3274	3000	2913			C—H stretching (methyl group)
9	3102	3272	2987	2912	2989		C—H stretching (methyl group)
10	3034	3189	2921	2838			C—H stretching (methyl group)
11	3034	3189	2921	2838			C—H stretching (methyl group)
12	3030	3188	2917	2837			C—H stretching (methyl group)
13	3091	3237	2976	2880		3008	C—H stretching (piperazine ring)
14	3088	3195	2973	2843			C—H stretching (piperazine ring)
15	3087	3195	2972	2843			C—H stretching (piperazine ring)
16	3050	3212	2937	2858			C—H stretching (piperazine ring)
17	3109	3203	2993	2850	2966	2966	C—H stretching (methylene)
18	3039	3252	2926	2894	2938		C—H stretching (piperazine ring)
19	3028	3240	2915	2883			C—H stretching (piperazine ring)
20	3044	3265	2931	2905			C—H stretching (methylene)
21	2925	3106	2816	2764			C—H stretching (piperazine ring)
22	2912	3094	2804	2753	2832	2848	C—H stretching (piperazine ring)
23	1642	1647	1581	1465	1602	1601	C—C stretching
24	1505	1524	1449	1356	1546		N—H in-plane bending
25	1488	1482	1432	1318	1477		C—C stretching
26	1468	1467	1413	1305	1456	1449	C—H in-plane bending
27	1381	1362	1329	1212	1363		C—H in-plane bending/N—C stretching
28	1313	1290	1264	1148	1289	1289	C—H in-plane bending/C—C stretching/C—N stretching
29	1254	1245	1207	1108	1235		C—C stretching
30	1213	1219	1168	1084	1210		C—H out-of-plane bending/CNC bending
31	1184	1175	1140	1045	1168	1168	C—O stretching
32	1110	1075	1068	956	1070	1074	C—H out-of-plane bending
33	1064	1043	1024	928	1040	1041	O—CH_3 stretching
34	958	965	922	858	950		C—H out-of-plane bending
35	894	893	860	794	892		N—H out-of-plane bending
36	847	879	815	782	858		C—H out-of-plane bending/N—H bending
37	820	840	789	747	832	831	C—O stretching
38	708	704	681	626	692		Ring deformation
39	664	648	639	576	669	669	CCN bending
40	572	578	550	514	578	578	CNC bending
41	525	538	505	478	547	548	CCO bending

mode of vibrations obtained by the RHF method is lower than the experimental results after scaling the frequencies (Table 2).

4.2.4 *C—C and C—N vibrations*

The identification of C—N vibrations is a difficult task because the mixing of vibrations is possible in this region. The FT-IR bands at 1363 and 1289 cm^{-1} and FT-Raman band at 1289 cm^{-1} are assigned to C—N stretching vibrations. This assignment was made in analogy with the literature [25,26]. The ring C—C stretching vibrations occur in the region 1625–1430 cm^{-1}. The FT-IR bands in the region 1602–1235 cm^{-1} and FT-Raman band at 1601 cm^{-1} in the spectra for the title molecule are assigned to C—C stretching vibrations. The CCN, CNC and CCC deformation vibrations traced in the lower wave number regions are identified and presented in the Table 2.

4.3 *^{1}H NMR spectral analysis*

The ^{1}H NMR spectrum simulated theoretically with the aid of ChemDraw Ultra 8.0 software program is shown in Figure 4. Table 4 gives the predicted chemical shift values obtained by the RHF, DFT and ChemDraw Ultra 8.0 software package and its assignment along with the shielding values. In general, highly shielded electrons appear downfield and vice versa. The present study reveals that the theoretically predicted chemical shifts slightly deviate from the experimental values. However,

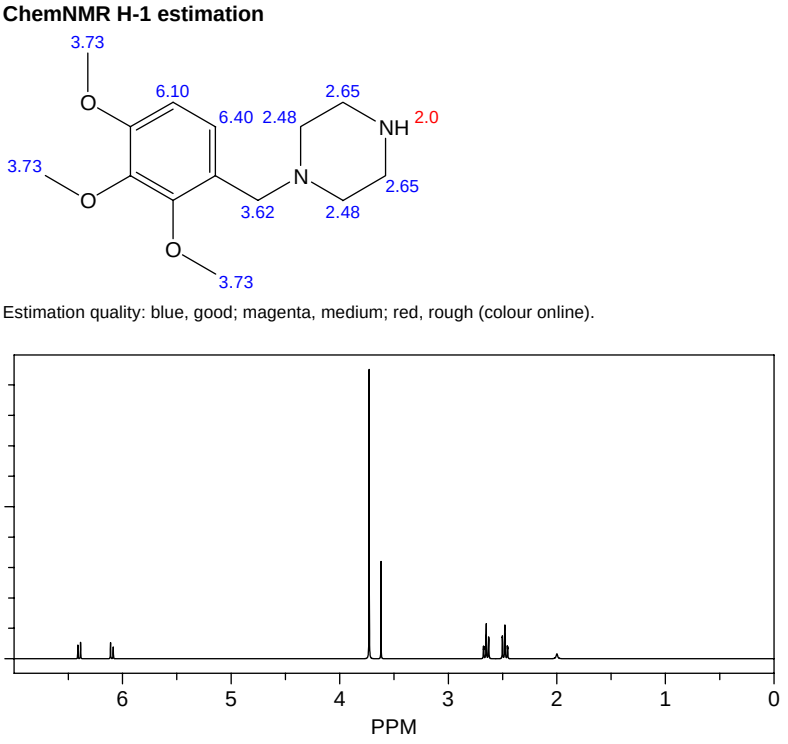

Estimation quality: blue, good; magenta, medium; red, rough (colour online).

Protocol of the H-1 NMR Prediction:

Node	Shift	Base + Inc.	Comment (ppm rel. to TMS)
CH2	2.48	1.37	methylene
		1.03	1 alpha -N(C)C
		0.08	1 beta -N-C
CH2	2.65	1.37	methylene
		1.22	1 alpha -N-C
		0.06	1 beta -N(C)C
NH	2.0	2.00	amine
CH2	2.65	1.37	methylene
		1.22	1 alpha -N-C
		0.06	1 beta -N(C)C
CH2	2.48	1.37	methylene
		1.03	1 alpha -N(C)C
		0.08	1 beta -N-C
CH2	3.62	1.37	methylene
		1.22	1 alpha -1:C*C*C*C*C*C*1
		1.03	1 alpha -N(C)C
CH	6.10	7.26	1-benzene
		-0.12	1 -C
		-0.44	1 -O-C
		-0.11	1 -O-C
		-0.49	1 -O-C
CH	6.40	7.26	1-benzene
		-0.20	1 -C
		-0.11	1 -O-C
		-0.44	1 -O-C
		-0.11	1 -O-C
CH3	3.73	0.86	methyl
		2.87	1 alpha -O-1:C*C*C*C*C*C*1
CH3	3.73	0.86	methyl
		2.87	1 alpha -O-1:C*C*C*C*C*C*1
CH3	3.73	0.86	methyl
		2.87	1 alpha -O-1:C*C*C*C*C*C*1

Figure 4. Theoretical ^{1}H NMR spectrum of TMZ.

it is observed that the predicted chemical shift values by the RHF method are in close agreement with the reported literature values. The spectrum of TMZ showed a singlet at 2.0 ppm for the proton of the amine hydrogen (H24) which contradicts the theoretical calculations. Both RHF and DFT methods which give the negative chemical shift values -0.09 and -0.5, respectively, for the amine hydrogen atom fail to predict the experimental values. Another singlet observed at δ 3.62 ppm for the methylene hydrogen atoms (H29 and H30) by ChemDraw Ultra fairly agrees with the RHF chemical shift values (3.9–4.6 ppm). This higher chemical shift is mainly due to bulky benzene

Table 4. Calculated and experimental proton NMR chemical shifts for TMZ.

Hydrogen atoms	Absolute shielding (ppm)	Calculated chemical shift (ppm)			Experimental chemical shift (ppm)[27,28]
		RHF	B3LYP	ChemDraw Ultra	
H20	29.46	2.5	3.1	2.48	2.67–2.74[28]
H21	28.96	3.1	3.6	2.48	
H22	28.92	3.1	3.6	2.65	2.67–2.74[28]
H23	28.65	3.4	3.9	2.65	
H24	32.68	−0.5	−0.09	2.0	
H25	28.90	3.1	3.6	2.65	2.67–2.74[28]
H26	28.61	3.4	3.9	2.65	
H27	29.32	2.7	3.2	2.48	
H28	29.26	2.6	3.3	2.48	
H29	28.15	3.9	4.4	3.62	
H30	27.39	4.6	5.1	3.62	
H31	24.60	7.9	7.9	6.10	6.5[27]
H32	24.71	7.8	7.8	6.40	
H33	27.65	4.5	4.9	3.73	3.79–3.89 [27], 3.84–3.86[27]
H34	28.04	4.0	4.5	3.73	
H35	28.13	3.9	4.4	3.73	
H36	27.63	4.5	4.9	3.73	
H37	27.79	4.2	4.8	3.73	
H38	27.65	4.3	4.9	3.73	
H39	27.49	4.5	5.1	3.73	
H40	28.25	3.7	4.3	3.73	
H41	27.61	4.5	4.9	3.73	

and piperazine ring groups. From the table, it is concluded that H29 atom is more shielded than H30 hydrogen atoms. Two triplet peaks at 2.48 and 2.65 ppm mark the methylene group hydrogen atoms in the piperazine ring. The hydrogen atoms in the methoxy groups appearing at higher chemical shift of 3.73 ppm are due to electronegative oxygen atoms. Also, another two doublet peaks at 6.1 and 6.4 ppm mark the aromatic hydrogen atoms, i.e. in the benzene ring. It is concluded that the predicted chemical shift values of RHF are in closer agreement with the experimental chemical shift values of the structurally related molecules [27,28].

4.4 UV spectral analysis

Electronic transition energies and oscillator strengths of TMZ were calculated employing both the ZINDO and time-dependent DFT (TD-DFT) methods for which the optimised geometry obtained from DFT calculations was used. The results of the theoretical calculations of electronic transition energies along with the band assignments are presented in Table 5, and they were compared with the experimental data of TMZ in *n*-hexane. The present experiment revealed two absorption bands at 270.4 and 215.2 nm in the UV region. The experimental and theoretical studies of the electronic absorption

Table 5. Assignment of observed electronic transitions.

S. no.	B3LYP				RHF				λ Exp. (nm)
	λ calc. (nm)	Energy (eV)	Oscillator strength *f*	State transitions	λ calc. (nm)	Energy (eV)	Oscillator strength *f*	State transitions	
1	272.12	4.5562	0.0349	H − 1 → L H → L	293.86	4.2192	0.0034	H − 1 → L H − 1 → L + 1 H → L H → l + 1	270.4
2	260.69	4.7559	0.0022	H − 2 → L H − 1 → L + 1 H → L + 1	260.50	4.7594	0.0029	H − 1 → L H − 1 → L + 1 H → L H → l + 1	
3	245.18	5.0569	0.0064	H − 3 → L + 1 H − 2 → L H → L + 1 H → L + 1(11%)	227.30	5.4546	0.7409	H − 4 → L + 2 H − 1 → L H → L + 1 H → L H → L + 1	215.2

Table 6. Theoretically calculated rotational constant, zero-point vibrational energy (ZPVE), entropy (cal/mol K), heat capacity (cal/mol K), thermal energy (kcal/mol), dipole moment, HOMO, LUMO and energy gap of TMZ.

Thermodynamic parameters	B3LYP/6-31G(d,p)	RHF/6-31G(d,p)
Rotational constant (GHz)	0.6401	0.6499
	0.2180	0.2198
	0.1928	0.1936
ZPVE (kcal/mol)	222.398	238.378
Entropy		
Total	143.881	141.355
Translational	42.636	42.636
Rotational	33.743	33.719
Vibrational	67.502	65.001
Heat capacity	72.725	67.650
Thermal energy	234.536	249.944
HOMO (eV)	5.2741	8.570
LUMO (eV)	0.0021	3.943
Energy gap (eV)	5.27	12.513

spectrum of TMZ were used to explain each observed band, which was not done earlier. Both the theoretical methods typically overestimate the observed electronic absorption bands of TMZ. However, the TD-DFT method electronic absorption bands calculated employing the closely agrees with the experimental results than with those of the ZINDO methods. The calculated thermodynamic parameters at room temperature are presented in Table 6. The DFT-calculated thermodynamic parameters are underestimated with RHF values. According to Koopman's theorem, ionisation potential is the negative of the highest occupied molecular orbital (HOMO) energy and affinity potential is the negative of the lowest unoccupied molecular orbital (LUMO) energy, and both are summarised in Table 6. From Table 6, it is concluded that the energy gap predicted by the DFT method is lower than that predicted by RHF method. The energy gap values show that the absence of inter- and intra-molecular charge transfer in TMZ molecule.

4.5 Chemical reactivity

Electron density is a property that contains all the information about the molecular system [29] and plays an important role in calculating electronegativity, chemical potential, electron affinity and ionisation potential. Parr and Yang [30] proposed a finite difference approach to calculate Fukui function indices, i.e. nucleophilic, electrophilic and radical attacks. In order to solve the negative Fukui function problem, different attempts were made by various groups [31–33]. Kolandaivel et al. [34] introduced the atomic descriptor to determine the local reactive sites of the molecular system. In the present study, the individual atomic charges calculated by MPA were used to calculate Fukui function and local softness for electrophilic and nucleophilic attacks. Table 7 shows the gross atomic charges, Fukui functions at the *k*th atom and local softness values for the title molecule calculated by MPA gross charges at both AM1 and PM3 level of calculation for which DFT-optimised geometry was used. The AM1-calculated Mulliken atomic charge has over-estimated values than the of PM3-calculated charge. These data would be used to explain the preferred position

Table 7. Atomic charges, Fukui functions (f_k) and local softness values for TMZ.

	AM1					PM3					Charge ratio
Atoms	Charge	f_k^+	f_k^-	$s_k^+f_k^+$	$s_k^-f_k^-$	Charge	f_k^+	f_k^-	$s_k^+f_k^+$	$s_k^-f_k^-$	(AM1/PM3)
N1	−0.2489	0.2969	0.0052	0.9699	0.0003	−0.0700	0.5425	0.0370	3.2369	0.0151	3.555
C2	−0.1027	−0.0632	0.0075	0.0440	0.0006	−0.1069	−0.0939	0.0060	0.1077	0.0004	0.960
C3	−0.0883	0.0148	0.0027	0.0024	0	−0.0921	−0.0077	−0.0040	0.0007	0.0002	0.958
N4	−0.2746	−0.0133	0.0072	0.0020	0.0006	−0.0592	0.0392	0.0230	0.0169	0.0058	4.638
C5	−0.0861	0.0102	0.0035	0.0011	0.0001	−0.0910	−0.0076	−0.0040	0.0006	0.0002	0.946
C6	−0.1074	−0.0584	0.0030	0.0375	0.0001	−0.1084	−0.1029	0.0059	0.1165	0.0004	0.990
C7	−0.0169	−0.0162	−0.0370	0.0029	0.0152	−0.0226	−0.0429	−0.0750	0.0203	0.0626	0.747
C8	−0.1637	−0.0470	0.1549	0.0243	0.2640	−0.1279	−0.1423	0.2593	0.2228	0.7394	1.279
C9	0.1159	−0.1130	0.0366	0.0014	0.0148	0.0639	0.0796	0.0469	0.0697	0.0242	1.813
C10	−0.0472	0.0326	0.0206	0.0117	0.0046	0.0252	−0.0577	0.0141	0.0367	0.0022	−1.873
C11	0.0922	0.0222	0.2687	0.0054	0.7939	0.0497	0.1079	0.2355	0.1279	0.6102	1.855
C12	−0.2293	0.0215	−0.1160	0.0051	0.1486	−0.1253	−0.0793	0.0311	0.0692	0.0107	1.830
C13	−0.0687	0.0138	0.1089	0.0021	0.1305	−0.0845	0.0775	0.0120	0.0660	0.0016	0.813
O14	−0.2037	0.0131	0.0197	0.0019	0.0043	−0.2059	0.0460	−0.0160	0.0233	0.0027	0.989
C15	−0.0774	−0.0067	−0.0005	0.0050	0	0.0589	−0.0140	0.0146	0.0022	0.0024	−1.314
O16	−0.2168	0.0050	−0.0113	0.0003	0.0014	−0.1873	0.0041	0.0148	0.0002	0.0024	1.157
C17	−0.0770	−0.0045	−0.0060	0.0002	0.0003	0.0440	−0.0049	−0.0010	0.0003	0	−1.750
O18	−0.2147	−0.0388	0.0260	0.0165	0.0074	−0.1969	−0.0382	0.0112	0.0161	0.0014	1.090
C19	−0.0656	−0.0008	−0.0040	0	0.0002	0.0429	0.0100	0.0002	0.0011	0	−1.529

of nucleophilic or electrophilic attack of this molecule. From Table 7, one can find that the complexities associated with f_k values due to the negative values were removed in the (*sf*) *k* values. It has been found that both AM1 and PM3 methods predict that the nitrogen atom, N1, has higher f_k^+ and $s_k^+ f_k^+$ values for nucleophilic attack. The order of electrophilic site as obtained by AM1 method is C11 > C8, whereas by PM3 method it is C8 > C11. Table 7 also gives the charge ratio which indicates the non-consistency between the two methods (AM1 and PM3).

5. Conclusion

We presented results of the structural and vibrational properties of TMZ using mid-IR and Raman spectra. The theoretically calculated values of both the bond lengths and bond angles of the structures of the minimum energy were then compared with X-ray crystallographic data. The data obtained during the course of the present investigation show that a better agreement between the experimental and computed data is obtained using the DFT method B3LYP, with the basis set 6-31G(d,p). This study predicted that the vibrational frequencies of TMZ could be successfully elucidated by the RHF and B3LYP methods using Gaussian program. The fitting between calculated and measured vibrational frequencies was achieved by these methods and the deviations between calculated and experimental values are quite small. Therefore, this study confirms that the theoretical calculation of the vibrational frequencies for TMZ is quite useful for determining the vibrational assignment and for predicting new vibrational frequencies. The calculated normal-mode vibrational frequencies provide thermodynamic properties by way of statistical mechanics. The individual atomic charges calculated by MPA were used to calculate the Fukui function to explain the chemical selectivity or reactivity site in TMZ.

Note

1. Presently Registrar, Periyar University, Salem, TN, India

References

[1] A. Onay-Besikci and S.A. Ozkan, *Trimetazidine revisited: A comprehensive review of the pharmacological effects and analytical techniques for the determination of trimetazidine*, Cardiovasc. Ther. 26 (2008), pp. 147–165.

[2] S. Dalla-Volta, G. Maraglino, P. Della-Valentina, P. Viena, and A. Desicleri, *A comparision of trimetazidine with nifedipine in effort angina: A double blind, crossover study*, Cardiovasc. Drugs Ther. 4 (1990), pp. 853–860.

[3] J.M. Detry, P. Sellier, S. Pennatorte, D. Cokkinos, H. Dargie, and P. Mathew, *Trimetazidine: A new concept in the treatment of angina. Comparison with propranolol in patients with sable angina*, Br. J. Clin. Pharmacol. 37(3) (1994), pp. 279–288.

[4] P. Sellier, C. Garpey, P. Corona, P. Andouin, and P. Ourbak, *Acute effects of trimetazidine on ergometric parameters in effort angina*, Cardiovasc. Drugs Ther. 4 (1990), pp. 820–821.

[5] N. Lavanchy, J. Martin, and A. Rossi, *Anti-ischaemic effects of trimetazidine: 31P-NMR spectroscopy in the study of isolated rat heart*, Arch. Int. Pharmacodyn. 286(1) (1987), pp. 97–110.

[6] R.F. Boucher, D.J. Hearse, and L.H. Opie, *Effects of trimetazidine on ischaemic contracture in isolated perfused rat hearts*, J. Cardiovasc. Pharmacol. 24(1) (1994), pp. 45–49.

[7] I. Inci, A. Dutly, D. Inci, A. Boehler, and W. Weder, *Recipient treatment with trimetazidine improves graft function and protects energy status after lung transplantation*, J. Heart Lung Transplant. 20(10) (2001), pp. 1115–1122.

[8] G. Kober, T. Bucke, H. Sievert, and C. Vallbracht, *Myocardial protection during percutaneous transluminal coronary angioplasty effects of trimetazidine*, Eur. Heart J. 13 (1992), pp. 1109–1115.

[9] J.N. Fabiani, O. Ponzio, S. Massonet-Castel, M. Paris, P. Chevalier, V. Jebara, and A. Carpentier, *Cardioprotective effect of trimetazidine during coronary artery graft surgery*, J. Cardiovasc. Surg. 33 (1992), pp. 486–491.

[10] P. Sellier, P. Audouin, B. Payen, P. Corona, T.C. Duory, and P. Ourbak, *Acute effects of trimetazidine evaluated by exercise testing*, Eur. J. Clin. Pharmacol. 33 (1987), pp. 205–207.

[11] M.J. Frisch, G.W. Trucks, H.B. Schlegel, G.E. Scuseria, M.A. Robb, J.R. Cheeseman, J.A. Montgomery, Jr, T. Vreven, K.N. Kudin, J.C. Burant, J.M. Millam, S.S. Iyengar, J. Tomasi, V. Barone, B. Mennucci, M. Cossi, G. Scalmani, N. Rega, G.A. Petersson, H. Nakatsuji, M. Hada, M. Ehara, K. Toyota, R. Fukuda, J. Hasegawa, M. Ishida, T. Nakajima, Y. Honda, O. Kitao, H. Nakai, M. Klene, X. Li, J.E. Knox, H.P. Hratchian, J.B. Cross, C. Adamo, J. Jaramillo, R. Gomperts, R.E. Stratmann, O. Yazyev, A.J. Austin, R. Cammi, C. Pomelli, J.W. Ochterski, P.Y. Ayala, K. Morokuma, G.A. Voth, P. Salvador, J.J. Dannenberg, V.G. Zakrzewski, S. Dapprich, A.D. Daniels, M.C. Strain, O. Farkas, D.K. Malick, A.D. Rabuck, K. Raghavachari, J.B. Foresman, J.V. Ortiz, Q. Cui, A.G. Baboul, S. Clifford, J. Cioslowski, B.B. Stefanov, G. Liu, A. Liashenko, P. Piskorz, I. Komaromi, R.L. Martin, D.J. Fox, T. Keith, M.A. Al-Laham, C.Y. Peng, A. Nanayakkara, M. Challacombe, P.M.W. Gill, B. Johnson, W. Chen, M.W. Wong, C. Gonzalez, and J.A. Pople, *Gaussian 03*, *Revision A.1*, Gaussian, Inc., Pittsburgh, PA, 2003.

[12] A.D. Becke, *Density-functional thermochemistry. III. The role of exact exchange*, J. Chem. Phys. 98 (1993), pp. 5648–5652.

[13] C. Lee, W. Yang, and R.G. Parr, *Development of the Colle–Salvetti correlation-energy formula into a functional of the electron density*, Phys. Rev. B37 (1988), pp. 785–789.

[14] Chem3D Ultra 8.0, Cambridgesoft.com, Cambridge, MA, USA.

[15] W. Yang and W. Mortier, *The use of global and local molecular parameters for the analysis of the gas-phase basicity of amines*, J. Am. Chem. Soc. 108 (1986), p. 5708.

[16] R.G. Parr and W. Yang, *Density Functional Theory of Atoms and Molecules*, Oxford University Press, Oxford, 1989.

[17] R. Tanaka, M. Haramura, A. Tanaka, and N. Hirayama, *Structure of trimetazidine*, Anal. Sci. 21 (2005), pp. x3–x4.

[18] A.P. Scott and L. Radom, *Harmonic vibrational frequencies: An evaluation of Hartree–Fock, Møller–Plesset, quadratic configuration interaction, density functional theory, and semiempirical scale factors*, J. Phys. Chem. 100(41) (1996), pp. 16502–16513.

[19] G. Socrates, *Infrared and Raman Characteristic Group Frequencies, Tables and Charts*, 3rd ed., Wiley, Chichester, UK, 2001.

[20] G. Fogarasi, X. Zhou, P.W. Taylor, and P. Pulay, *The calculation of* ab initio *molecular geometrics: efficient optimization by natural internal coordinates and empirical corrections by offset forces*, J. Am. Chem. Soc. 114 (1992), p. 8191.

[21] L.J. Bellamy, *The Infrared Spectra of Complex Molecules*, John Wiley, New York, 1956.

[22] V. Krishnakumar and S. Seshadri, *Scaled quantum chemical calculations and FT-IR, FT-Raman spectral analysis of 2-methylpiperazine*, Spectrochim. Acta A 68 (2007), pp. 833–838.

[23] B. Lakshmaiah and G.R. Rao, *Vibrational analysis of substituted anisoles. I-Vibrational spectra and normal coordinate analysis of some fluoro and chloro compounds*, J. Raman Spectrosc. 20 (1989), p. 439–448.

[24] R.M. Silverstein, G. Clayton Bassler, and T.C. Morril, *Vibrational spectroscopy investigation using* ab initio *and density functional theory analysis on the structure of 2-amino-4,6-dimethoxypyrimidine*, *Spectrometric Identification of Organic Compounds*, 5th ed., John Wiley & Sons, New York, 1991.

[25] N. Sundaraganesan, K.S. Kumar, C. Meganathan, and B.D. Joshua, *Vibrational spectroscopy investigation using ab initio and density functional theory analysis on the structure of 2-amino-4,6-dimethoxypyrimidine*, Spectrochim. Acta A 65 (2006), p. 1186.

[26] V. Krishnakumar and R. Ramasamy, *Scaled quantum chemical studies of the structure and vibrational spectra of 2-(methyl thio)benzimidazole*, Spectrochim. Acta A 62 (2005), p. 570.

[27] V. Srivastava, A.S. Negi*, J.K. Kumar, U. Faridi, B.S. Sisodia, M.P. Darokar, S. Luqman, and S.P.S. Khanuja, *Synthesis of 1-(30,40,50-trimethoxy) phenyl naphtho[2,1b]furan as a novel anticancer agent*, Bioorg. Med. Chem. Lett. 16 (2006), pp. 911–914.

[28] H. Fukushi, H. Mabuchi, Z. Terashita, K. Nishikawa, and H. Sugihara, *Synthesis and platelet activating factor (APF)-antagonistic activities of tri substituted piperazine derivatives*, Chem. Pharm. Bull. 42(3) (1994), pp. 551–559.

[29] W. Yang and R.G. Parr, *Hardness, softness and the Fukui function in the electronic theory of metals and catalysis*, Proc. Natl Acad. Sci. USA 82 (1985), pp. 6723–6726.

[30] R.G. Parr and W. Yang, *Density functional approach to the frontier-electron theory of chemical reactivity*, J. Am. Chem. Soc. 106 (1984), pp. 4049–4050.

[31] R.K. Roy, K. Hirao, S. Krishnamurthy, and S.J. Pal, *Mulliken population analysis based evaluation of condensed Fukui function indices using fractional molecular charge*, J. Chem. Phys. 118 (2001), pp. 2901–2907.

[32] P. Bultinck, R. Carbo-Dorca, and W.J. Langenaeker, *Negative Fukui function: New insights based on electronegativity equalizations*, J. Chem. Phys. 34 (2003), pp. 4349–4356.

[33] P. Butlinck and R.J. Carbo-Dorca, *Negative and infinite Fukui functions: The role of diagonal dominance in the hardness matrix*, J. Math. Chem. 34 (2003), pp. 67–74.

[34] P. Kolandaivel, G. Praveena, and P. Selvarengan, *Study of atomic and condensed atomic indices for reactive sites of molecules*, J. Chem. Sci. 117(5) (2005), pp. 591–598.